A Multiple-endpoints Chebysheve Collocation Method for High Order Differential Equations‡

Shan Wang and Zhiping Li†

Abstract. A new collocation method with multiple-endpoints and a new boundary condition technique is established for high order differential equations. Numerical examples on 1D sixth order and 2D fourth order linear problems show that the new method efficiently improves the condition numbers and the convergence rates. An example on nonlinear elastic thin film buckling shows the advantage of the new method for high order nonlinear partial differential equations with complex boundary conditions.

1. Introduction

Pseudospectral methods as meshless methods are successfully used for widely diverse applications [**1**]. The Chebyshev type collocation methods are among the most popular spectral methods because of computational convenience [**2**]. A typical choice of collocation points for solving boundary value problems of second order differential equations with a Chebyshev method is to use the Chebyshev-Gauss-Lobatto collocation points, which include certain inner collocation points and two end points. Chebyshev-Gauss collocation method, which has no endpoints, is also a popular choice. However, difficulties arise when pseudospectral method is applied to higher order differential equations, especially in high dimensions [**2**], for example it usually leads to an over-determined system. There are two standard ways to deal with the problem (Chapter 6 in [**2**]). One is to use either more base functions [**2**] or less inner collocation points [**3**] with a shortcoming that the condition number is typically very large. The other is to introduce proper variable substitutions so that part of the boundary conditions are satisfied naturally by the new unknown functions (e.g. [**4**]). However, for complicated boundary conditions, such as reciprocally periodic connection boundary conditions [**5**] and nonlinear boundary conditions [**6**], it can hardly work.

In this paper, we designed a new multiple-endpoints collocation points for high order differential equations. Numerical examples on 1D 6th-order and 2D 4th-order linear differential equations are presented to show the improved condition numbers of the differential matrices and better accuracy of the new method. In particular,

---

2010 *Mathematics Subject Classification.* 65N35, 65L60.

Key words and phrases. Chebyshev collocation method, multiple-endpoints, high order partial differential equations, complex boundary conditions.

†Corresponding author: Zhiping Li, email address: lizp@math.pku.edu.cn.

‡The research was supported by the NSFC project 11171008 and RFDP of China.

we present an example on an elastic thin film buckling problem governed by a nonlinear von Kárman equation, for which the standard Chebyshev methods failed to produce physically consistent solutions.

The rest of the paper is organized as follows. The new multiple-endpoints collocation points and the new boundary condition technique are introduced in Section 2. In Section 3, the numerical results are presented, discussed, and comparisons are made. The paper ends with some concluding remarks in Section 4.

2. Multiple-endpoints Collocation Points

2.1. The base functions of multiple-endpoints collocation method and the corresponding collocation points. Let T_n be the Chebychev polynomial with degree n and $\omega(x)$ be the corresponding weight function [**1**]. Follow the theory of Gauss-Lobatto collocation points [**1**], we consider polynomials

$$Q_{N+1,m}(x) = T_{N+1}(x) + \sum_{k=1}^{2m} a_{N+1,k} T_{N+1-k}(x), \quad N+1 \geq 2m, \tag{2.1}$$

where $\{a_{N+1,k}\}_{k=1}^{2m}$ are so taken that $Q_{N+1,m}^{(s)}(\pm 1) = 0$, $s = 0, 1, \cdots, m-1$.

Two of the most important properties of the polynomials $\{Q_{N,m}\}_{N=2m}^{\infty}$ are revealed by the following two theorems, i.e. for certain properly chosen weight, they are a sequence of orthogonal polynomials, and their zeros in $(-1,1)$ are simple and are the corresponding Gauss quadrature points.

THEOREM 2.1. *The polynomials* $\{\frac{Q_{N,m}}{(1-x^2)^m}\}_{N=2m}^{\infty}$ *are orthogonal in* $L^2_{\omega_m}(-1,1)$ *with the weight* $\omega_m(x) = (1-x^2)^m \omega(x) = (1-x^2)^{m-\frac{1}{2}}$.

As a consequence of Theorem 2.1, it can be shown that the polynomial $Q_{N+1,m}(x)$ has $N+1-2m$ separated simple zeros in $(-1,1)$ (see Lemma 1.2.2 in [**1**] page 10) and two m-zeros at each of the boundary points.

Let $x_0 = x_1 = \cdots = x_{m-1} = -1, x_{N+1-m} = \cdots = x_{N-1} = x_N = 1$ and $-1 < x_m < \cdots < x_{N-m} < 1$ be the $N+1$ roots of the polynomial $Q_{N+1,m}$ given by (2.1), we call $\{x_i\}_{i=0}^{N}$ the multiple-endpoints Chebychev collocation points.

THEOREM 2.2. *Let* $-1 < x_m < x_{m+1} < \cdots < x_{N-m} < 1$ *be the* $N+1-2m$ *zeros of the polynomial* $\frac{Q_{N+1,m}}{(1-x^2)^m}$. *Let* $\{w_m^{N+1,m}, w_{m+1}^{N+1,m}, \cdots, w_{N-m}^{N+1,m}\}$ *be the corresponding quadrature weights for the integral* $\int_{-1}^{1} p(x)\omega_m(x)dx$ *with weight* $\omega_m(x) = (1-x^2)^{m-\frac{1}{2}}$. *Then, we have* $w_j^{N+1,m} > 0$, $j = m, \cdots, N-m$, *and*

$$\sum_{j=m}^{N-m} p(x_j) w_j^{N+1,m} = \int_{-1}^{1} p(x)\omega_m(x)dx, \qquad \forall p \in \mathbb{P}_{2N-4m+1}.$$

By the expression (2.1), if the parameters $\{a_k\}_{k=1}^{2m}$ are given, the values of the polynomials $Q_{N+1,m}$ and their derivatives $Q_{N+1,m}^{(s)}$ can be easily calculated by working with the corresponding results of the Chebyshev polynomials. Substitute the boundary values of the Chebyshev polynomials [**1**] into the expression (2.1) of the polynomials $Q_{N+1,m}$, then the $2m$ boundary conditions $Q_{N+1,m}^{(s)}(\pm 1) = 0$, $s = 0, 1, \cdots, m-1$ give a linear system that the parameters $\{a_k\}_{k=1}^{2m}$ must satisfy. After some elementary manipulations with the equations, we are lead to the following linear systems $A\overrightarrow{a}_{odd} = \mathbf{0}, A\overrightarrow{a}_{even} = -(1, (N+1)^2, \cdots, (N+1)^{2(m-1)})^T$, where $\overrightarrow{a}_{odd} = (a_1, a_3, \cdots, a_{2m-1})^T$, $\overrightarrow{a}_{even} = (a_2, a_4, \cdots, a_{2m})^T$, and where the matrix $A := (A_{ij})_{i,j=1}^m$ with $A_{ij} = (N+1-2j)^{2i-2}$. Obviously, for $N > 2m$, A is a nonsingular Vandermonde matrix. Thus the parameteres $\{a_k\}_{k=1}^{2m}$ are uniquely solvable, and in particular, $\overrightarrow{a}_{odd} = \mathbf{0}$.

2.2. Discretization with Chebyshev Collocation Methods. Consider boundary value problems of differential equations of the form

$$\mathcal{L}u(x) = f(x) \quad x \in \Omega, \tag{2.2}$$

$$\mathcal{B}u(x) = g(x) \quad x \in \partial\Omega. \tag{2.3}$$

In 1D, for simplicity, let $\Omega = (-1, 1)$. Let k be the number of boundary conditions, let $\{x_i\}_{i=1}^{N+1-k} \subset (-1, 1)$ be the inner collocation points, and $\bar{x}_i \in \{-1, 1\}$, $1 \le i \le k$ be the multiple boundary collocation points corresponding to the boundary conditions. Substituting $u_N(x) = \mathbf{T}_N(x)\hat{\mathbf{U}}_N$ into (2.2) and (2.3), and evaluating at the collocation points, we obtain a system of $N+1$ equations for $N+1$ unknowns $\hat{\mathbf{U}}_N = (\hat{u}_0, \hat{u}_1, \cdots, \hat{u}_N)^T$:

$$\begin{pmatrix} \mathbf{T}_{in}^N L_N \\ \mathbf{T}_{br}^N \odot B_N \end{pmatrix} \hat{\mathbf{U}}_N = \begin{pmatrix} \mathbf{f}_{in} \\ \mathbf{g}_{br} \end{pmatrix}, \tag{2.4}$$

where $\mathbf{T}_{in}^N$ is a $(N+1-k) \times (N+1)$ matrix whose i-th row is $\mathbf{T}_N(x_i)$, $\mathbf{T}_{br}^N$ is a $k \times (N+1)$ matrix whose i-th row is $\mathbf{T}_N(\bar{x}_i)$, L_N is the differential matrix of the differential operators $\mathcal{L}$, $\mathbf{T}_{br}^N \odot B_N$ is a $k \times (N+1)$ matrix whose i-th row is given by $\mathbf{T}_N(\bar{x}_i)B_N^i$ with B_N^i being the differential operator of the differential operator $\mathcal{B}$ at $\bar{x}_i$, $\mathbf{f}_{in} = (f(x_1), \cdots, f(x_{N+1-k}))^T$ and $\mathbf{g}_{br} = (g(\bar{x}_1), \cdots, g(\bar{x}_k))^T$. The method works in a similar way for higher dimensions (see for example [**1**]).

Notice that, if $\mathcal{B}$ and $\mathcal{L}$ are linear, then instead of solving the system (2.4) for $\hat{\mathbf{U}}_N$, it could be more convenient to solve the following smaller system for $\bar{\mathbf{U}}_{in}$:

$$\mathbf{T}_{in}^N L_N S_1 \bar{\mathbf{U}}_{in} = \mathbf{f}_{in} - \mathbf{T}_{in}^N L_N S_2 \mathbf{g}_{br}, \tag{2.5}$$

where (S_1, S_2) is the inverse matrix of $\begin{pmatrix} \mathbf{T}_{in}^N \\ \mathbf{T}_{br}^N \odot B_N \end{pmatrix}$, *i.e.* $(S_1, S_2)\begin{pmatrix} \mathbf{T}_{in}^N \\ \mathbf{T}_{br}^N \odot B_N \end{pmatrix} = I$. The approach can also be extended to the case where $\mathcal{L}$ is nonlinear.

2.3. Solving problems with homogeneous boundary conditions. For a standard homogeneous boundary value problem of a $2k$th-order partial differential equation defined on $(-1, 1)$, we can use the $N+1-2k$ separated simple zeros of $Q_{N+1,k}$ as the inner collocation points, and find numerical solutions of the problem by solving the equations (2.4) or (2.5) with $\mathbf{g}_{br} = 0$.

Noticing that the polynomials $\{Q_{K,k}\}_{K=2k}^N$ are a set of base functions for the space of polynomials $\mathbb{Q}_N = \{p \in \mathbb{P}_N : p^{(j)}(\pm 1) = 0,\ j = 0, \cdots, k\}$, we may as well directly express the approximation solution as $u_N(x) = \mathbf{Q}_N(x)\tilde{\mathbf{U}}_N$, where $\mathbf{Q}_N(x) = (Q_{2k,k}, Q_{2k+1,k}, \cdots, Q_{N,k})$, and solve for $\tilde{\mathbf{U}}_N = (\tilde{u}_{2k}, \cdots, \tilde{u}_N)^T$. By (2.1), we have $\mathbf{Q}_N(x) = \mathbf{T}_N(x)\mathbf{A}^{N,k}$, where $\mathbf{A}^{N,k}$ is a $(N+1) \times (N+1-2k)$ matrix. This implies that $\hat{\mathbf{U}}_N = \mathbf{A}^{N,k}\tilde{\mathbf{U}}_N$. Thus, the discrete system (2.4) is transformed to an equivalent reduced system

$$\mathbf{T}_{in}^N L_N \mathbf{A}^{N,k} \tilde{\mathbf{U}}_N = \mathbf{f}_{in}. \tag{2.6}$$

The method can be naturally extended to solve homogeneous boundary value problems defined on the domain $(-1, 1)^d$ in d-dimensions.

2.4. Solving problems with inhomogeneous boundary conditions. For an inhomogeneous boundary value problem of a $2k$th-order linear partial differential equation defined on $(-1,1)$, we decompose the approximation solution $u_N(x) = \mathbf{T}_N(x)\hat{\mathbf{U}}_N$ into two parts, that is $u_N(x) = \mathbf{T}_N(x)(\hat{\mathbf{U}}_N^0 + \hat{\mathbf{U}}_N^1)$, where $\mathbf{T}_N(x)\hat{\mathbf{U}}_N^1$ satisfies the inhomogeneous boundary condition (see (2.4))

$$(\mathbf{T}_{br}^N \odot B_N)\hat{\mathbf{U}}_N^1 = \mathbf{g}_{br}, \tag{2.7}$$

and $\mathbf{T}_N(x)\hat{\mathbf{U}}_N^0$ satisfies the homogenous boundary condition and the equation

$$\mathbf{T}_{in}^N L_N \hat{\mathbf{U}}_N^0 = \mathbf{f}_{in} - \mathbf{T}_{in}^N L_N \hat{\mathbf{U}}_N^1. \tag{2.8}$$

Obviously, the above decomposition is not unique. For the sake of simplicity and stability, we determine $\hat{\mathbf{U}}_N^1$ by solving the equation (2.7) with the least square method, in which we require that the L^2 norm of $L_N\hat{\mathbf{U}}_N^1$ is minimized. Instead of solving (2.8), we solve, by the method given in §2.3 (see (2.6)), the equation

$$\mathbf{T}_{in}^N L_N \mathbf{A}^{N,k}\tilde{\mathbf{U}}_N^0 = \mathbf{f}_{in} - \mathbf{T}_{in}^N L_N \hat{\mathbf{U}}_N^1 \tag{2.9}$$

for the homogeneous part of the solution which is now given in the form $\mathbf{T}_N(x)\hat{\mathbf{U}}_N^0 = \mathbf{Q}_N(x)\tilde{\mathbf{U}}_N^0$. This approach can also be naturally extended to solve inhomogeneous boundary value problems defined on the domain $(-1,1)^d$ in d-dimensions.

Notice that, in the standard approaches for inhomogeneous boundary value problems in higher dimensions, the discrete equation, which is in general a underdetermined system because of the multi-counted boundary corner collocation points, is solved either by the least square method or by eliminating certain numbers of the highest order base polynomials. In contrast, our approach here produces in theory an exact solution which generally consists of all admissible base polynomials. In addition, our numerical experiments show that our method is more robust and can produce more accurate numerical solutions.

3. Numerical examples

3.1. 1D 6th-order linear problem. First, we consider a 6th-order linear problem with homogeneous boundary conditions:

$$\begin{cases} u^{(6)}(x) - u(x) = f(x), & -1 < x < 1, \\ u(\pm 1) = 0, u'(\pm 1) = 0, u''(\pm 1) = 0. \end{cases} \tag{3.1}$$

For simplicity of notations, we rewrite the linear equations (2.5) (for $\mathbf{g}_{br} = 0$) and (2.6) in the form $\mathbf{L}_N^1\bar{\mathbf{U}}_{in} = \mathbf{f}_{in}$ and $\mathbf{L}_N^0\tilde{\mathbf{U}}_N = \mathbf{f}_{in}$ respectively, where $\mathbf{L}_N^1 = \mathbf{T}_{in}^N L_N S_1$ and $\mathbf{L}_N^0 = \mathbf{T}_{in}^N L_N \mathbf{A}^{N,k}$. The condition numbers $\mathrm{cond}(\mathbf{L}_N^i)$ of the matrixes $\mathbf{L}_N^i$ corresponding to the Chebyshev-Gauss, Chebyshev-Gauss-Lobatto, and Chebyshev-Multiple-Endpoints collocation points are compared in the left subfigure of Figure 1, where it is seen that the Chebyshev-Multiple-Endpoints method has obviously much smaller condition numbers $\mathrm{cond}(\mathbf{L}_N)$.

To compare the accuracy of numerical solutions, let the exact solution be given by $u(x) = e^x + p(x)$ with $p(x) = f(x) \in \mathbb{P}_5$, and let $u_N^1(x) = \mathbf{T}_N(x)\hat{\mathbf{U}}_N = \mathbf{T}_N(x)S_1\bar{\mathbf{U}}_{in} \in \mathbb{P}_N(-1,1)$ be the numerical solutions obtained by solving $\mathbf{L}_N^1\bar{\mathbf{U}}_{in} = \mathbf{f}_{in}$ and $u_N^0(x) = \mathbf{Q}_N(x)\tilde{\mathbf{U}}_N \in \mathbb{P}_N(-1,1)$ be the numerical solutions obtained by solving $\mathbf{L}_N^0\tilde{\mathbf{U}}_N = \mathbf{f}_{in}$ respectively. In the right sub-figure of Figure 1, the error $e_u = \|u - u_N^i\|_{L^2(-1,1)}$ of the numerical solutions are compared, where we see that the new method has smaller error and reaches the machine accuracy faster than the other methods. It is also seen that u_N^0 reaches higher accuracy than u_N^1.

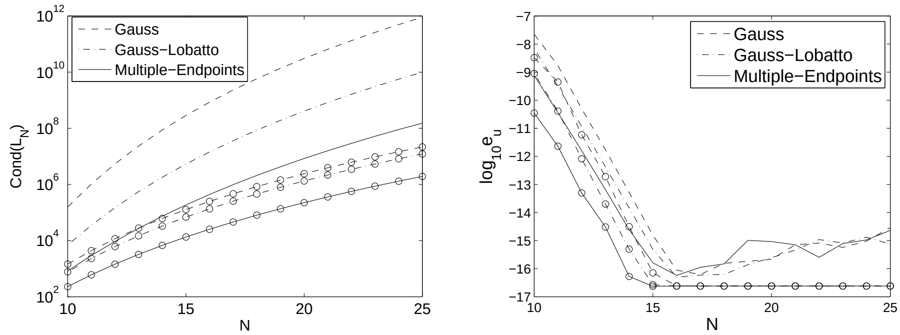

FIGURE 1. The numerical results of $\mathrm{cond}(\mathbf{L}_N^i)$ and e_u^i, $i = 0, 1$, where the results with respect to $i = 0$ are marked by $\circ$.

3.2. Biharmonic equation. Next, we consider the 2D biharmonic equation with clamped boundary conditions:

$$
\begin{cases} \Delta^2 u(x,y) = f(x,y), & (x,y) \in \Omega, \\ u(x,y) = g_0,\ \dfrac{\partial u}{\partial n}(x,y) = g_1, & (x,y) \in \partial\Omega. \end{cases} \tag{3.2}
$$

where Δ denotes the Laplace operator, and $\Omega = (-1,1)^2$.

We choose the same polynomial base functions for the two dimensions, and write the discrete solution in the form $u_N(x,y) = \sum_{i=0}^{N}\sum_{j=0}^{N} \hat{u}_{ij} T_i(x) T_j(y)$.

We consider homogenous and inhomogeneous boundary conditions seperately. We compare three types of collocation points, which are the Chebyshev-Gauss, Chebyshev-Gauss-Lobatto, and Chebyshev-Multiple-Endpoints collocation points. At the same time, the new boundary technique introduced in §2.3 and §2.4 (referred to as the first method in Figures 2 and 3) is compared with a standard method (referred to as the second method in Figures 2 and 3), in which the four highest order terms are omitted and the discrete solution is written as

$$
u_N(x,y) = \sum_{i=0}^{N}\sum_{j=0}^{N} \hat{u}_{ij} T_i(x) T_j(y) - \sum_{i=N-1}^{N}\sum_{j=N-1}^{N} \hat{u}_{ij} T_i(x) T_j(y). \tag{3.3}
$$

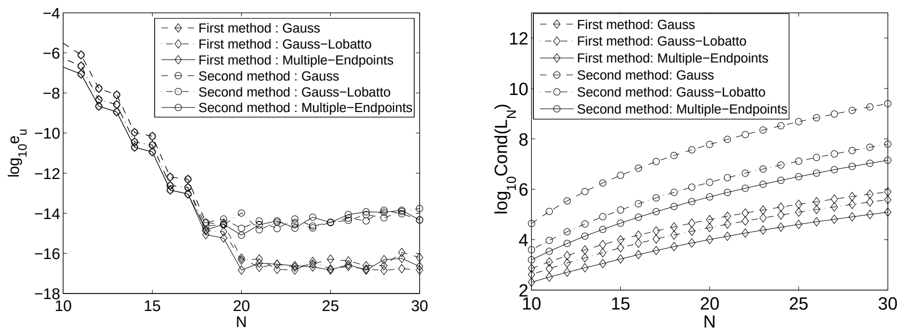

FIGURE 2. Numerical results for homogeneous problem.

The numerical results of homogenous case is shown in Figure 2, in which the exact solution is given by $u(x,y) = \pi^{-4}(1 + \cos(\pi x))(1 + \cos(\pi y))$. In the left sub-figure of Figure 2, the comparison of the error $e_u = \|u_N(x) - u(x)\|_{L^2(-1,1)^2}$ shows clearly that our boundary technique leads to higher accuracy. The numerical results of Multiple-Endpoints-Chebyshev collocation points are also seen to perform slightly better than the others. The numerical results on the condition number Cond(L_N) is shown in the right sub-figure of Figure 2, in which L_N corresponding to $\mathbf{T}_{in}^N L_N \mathbf{A}^{N,k}$in (2.6) for the first method and to $\mathbf{T}_{in}^N L_N S_1$ in (2.5) for second method. It is clearly seen that the Multiple-Endpoints-Chebyshev collocation points and the new boundary technique result in significantly lower condition numbers.

For the inhomogeneous case, we consider two exact solutions $u^1(x,y) = \pi^{-4}(1+\cos(\pi x))(1+\cos(\pi y)) + 0.1(y+1)$ and $u^2(x,y) = \ln(2+xy)+1$. The errors are shown in Figure 3. Obviously, the error of latter decrease much slower, this is not a surprise since the Fourier expansion of the latter converges much slower. The first method is still seen to work better than the second method, and the difference can be crucial sometimes. The advantage of Multiple-Endpoints-Chebyshev collocation points on the accuracy also appears to be more significant.

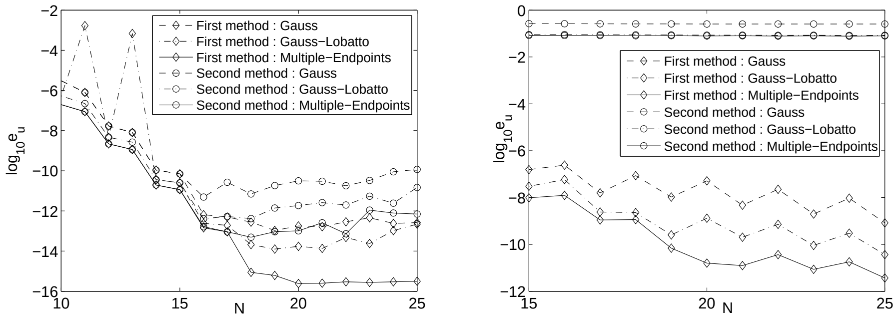

FIGURE 3. Numerical results for u^1 (on the left) and u^2 (on the right).

3.3. An example in thin film delamination. In this sunsection, we consider an example of telephone-cord buckling of elastic thin film [**7, 8**], which can be modeled by a nonlinear von Kárman plate equations [**5, 7, 8, 9, 10, 11**].

In the annular sector model [**5**], an equilibrium state of a buckle can be obtained by solving the following nonlinear dynamic system

$$\begin{cases} w_{,tt} + cw_{,t} + \triangle^2 w - \dfrac{4\pi^2}{(1-r_0)^2}\sigma_0 \triangle w - NLT_W(w,u,v) = 0, \\ LT_U(u,v) + NLT_U(w) = 0, \\ LT_V(u,v) + NLT_V(w) = 0, \end{cases} \tag{3.4}$$

defined on an annular sector region $\Omega = \{(r,\theta)|\, r_0 < r < 1, -\theta_0 < \theta < \theta_0\}$, where LT, NLT stand for the corresponding linear and nonlinear terms (see [**5**] for details). The system is coupled with the clamped boundary conditions on $r = r_0$ and $r = 1$:

$$\begin{cases} w(r_0,\theta) = 0,\ w_{,r}(r_0,\theta) = 0,\ u(r_0,\theta) = 0,\ v(r_0,\theta) = 0, \\ w(1,\theta) = 0,\ \ w_{,r}(1,\theta) = 0,\ \ u(1,\theta) = 0,\ \ v(1,\theta) = 0, \end{cases} \tag{3.5}$$

and the reciprocally periodic connection boundary conditions on $\theta = -\theta_0$, θ_0:

$$
\begin{cases}
\frac{1}{r^k}\frac{\partial^k w}{\partial \theta^k}\Big|_{(r,-\theta_0)} = \frac{1}{(1+r_0-r)^k}\frac{\partial^k w}{\partial \theta^k}\Big|_{(1+r_0-r,\,\theta_0)}, \qquad k = 0,1,2,3, \\
u(r,-\theta_0) = -u(1+r_0-r,\theta_0), \ \frac{u_{,\theta}\,(r,-\theta_0)}{r} = -\frac{u_{,\theta}\,(1+r_0-r,\theta_0)}{1+r_0-r}, \\
v(r,-\theta_0) = v(1+r_0-r,\theta_0), \quad \frac{v_{,\theta}\,(r,-\theta_0)}{r} = \frac{v_{,\theta}\,(1+r_0-r,\theta_0)}{1+r_0-r}.
\end{cases} \tag{3.6}
$$

Map the normalized annular sector domain $\Omega = \{(r,\theta)\big| r_0 \le r \le 1,\ -\theta_0 \le \theta \le \theta_0\}$ onto the standard computational domain $\hat{\Omega} = \{(x,y)\big| -1 \le x \le 1,\ -1 \le y \le 1\}$ with $x = (2r-1-r_0)/(1-r_0)$, $y = \theta/\theta_0$. Rewrite the out-of-plane dimensionless displacement $w(x,y)$ in the form $w(x,y) = (1-x^2)q(x,y)$, so that the clamped boundary conditions (3.5) are naturally satisfied [**5**].

We use Chebyshev-Gauss-Lobatto collocation points in the last two equations of (3.4) for x and y and in the first equation of (3.4) for x, and test the three types of collocation points in the first equation of (3.4) for y. For time discretization, the Newmark-β method is used for the first equation in (3.4).

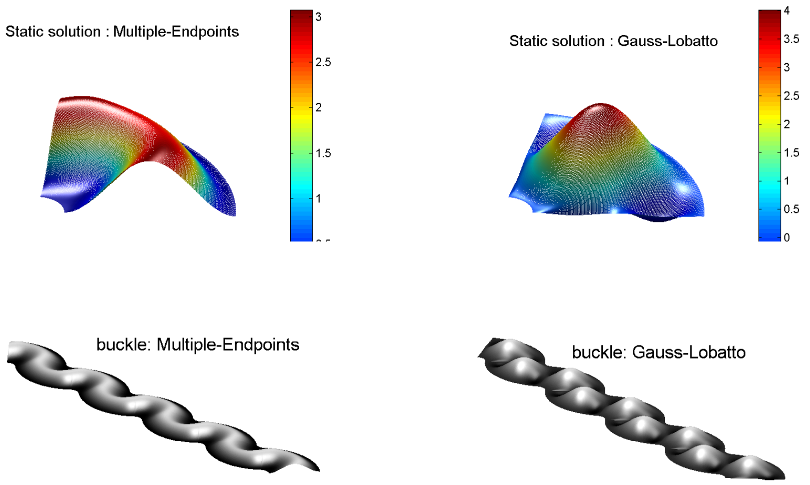

FIGURE 4. Numerical solutions and corresponding buckle morphologies.

For a set of physically relevant data $\sigma_0 = 10$, $r_0 = 0.15$, $\theta_0 = 0.7$, take small smooth functions $w_0 = 0.01(1-r)^2(r_0-r)^2, u_0 = 0, v_0 = 0$ as the initial state. Our numerical experiments showed that, while the scheme using the Chebyshev-Gauss collocation points always leads to blow up, the schemes using the other two types of collocation points can converge and produce static numerical solutions. The numerical solutions, with respect to $M = 20$, $N = 10$ and $c = 1000$, obtained by using the Multiple-Endpoints and Chebyshev-Gauss-Lobatto collocation points are shown in Figure 4.

Compare the numerical solutions with the physical experiments (see figures in [**9, 10, 11**], e.g. figure 1(c) in [**10**]), we see that the numerical results produced by using the Multiple-Endpoints fit the physical experiment well, while the numerical result produced by using the Chebyshev-Gauss-Lobatto collocation points is nonphysical with obvious negative values in the out-of-plane displacement.

4. Conclusions

The Chebyshev-Multiple-Endpoints collocation method and a new boundary condition technique are established in this paper for boundary value problems of high order differential equations. The new collocation points can be easily obtained by working with the Chebyshev polynomials. For linear problems, our numerical results showed that the new collocation points and the new boundary condition technique really helped to improve the condition numbers of differentiation matrices and the approximation accuracy of the numerical solutions. In particular, an example on nonlinear elastic thin film buckling showed that the improvement in the condition number can be crucial to the success of solving nonlinear problems.

References

[1] J. Shen, T. Tang, 2006, Spectral and high-order methods with applications, Science press, Beijing.
[2] J. P. Boyd, 1989, Chebyshev & Fourier spectral methods, Springer-Verlag Berlin, Heidelberg.
[3] C. Bernardi, G. Coppoletta, Y. Maday, 1992, Some spectral approximations of two-dimensional fourth-order problems, mathematics of computation 59, 63-67.
[4] R. M. Kirby and Z. Yosibash, 2004, Solution of von-Karman dynamic non-linear plate equations using a pseudo-spectral method, Computer Methods in Applied Mechanics and Engineering 193, 575-599.
[5] S. Wang and Z. P. Li, Mathematical modeling and numerical simulation of telephone cord buckles of elastic films, 2001, Science China Mathematics 54,1063-1076.
[6] J.F. Bonder, J.D. RossiExistence results for the p-Laplacian with nonlinear boundary conditions, 2001, Journal of Mathematical Analysis and Applications, 195-223.
[7] G. Gioia, M. Ortiz, 1997, Delamination of compressed thin films, Advances in Applied Mechanics 33, 119-192.
[8] L. B. Rreund and S. Suresh, 2003, Thin film materials: stress, defect formation, and surface evolution, Cambridge University Press.
[9] J. Colin, F. Cleymand, C. Coupean, J. Grilhe, 2000, Worm-like delamination patterns of thin stainless steel films on polycarbonate substrates. Philos. Mag. A 80 (11), 2559-2568.
[10] M. W. Moon, H. M. Jensen, J. W. Hutchinson, K. H. Oh, A. G. Evans, 2002, The characterization of tepephone cord buckling of compressed thin films on substrates, Journal of the Mechanics and Physics of Solids 50, 2355-2377.
[11] M. Cordill, D. Bahr, N. Moody, W. Gerberich, 2007, Adhesion measurements using telephone cord buckles, Materials Science and Engineering: A Volume 443, 150-155.

Shan Wang, LMAM & School of Mathematical Sciences, Peking University, Beijing 100871, P.R.China
E-mail address: shasti0@pku.edu.cn

Zhiping Li, LMAM & School of Mathematical Sciences, Peking University, Beijing 100871, P.R.China
E-mail address: lizp@math.pku.edu.cn